Section 4

Parameterization of important atmospheric and surface processes, effects of different parameterizations

Improvement of a Stratocumulus Scheme for Mid-latitude Marine Low Clouds

Hideaki Kawai
Meteorological Research Institute, Japan Meteorological Agency
(e-mail: h-kawai@mri-jma.go.jp)

1. Introduction

In the operational global model of the JMA (Japan Meteorological Agency); i.e., the GSM (Global Spectral Model), mid-latitude marine low clouds are not adequately represented, and there is a longstanding issue that shortwave radiation flux excessively penetrates into the mid-latitude oceans, especially during the summer. A similarly serious excess shortwave radiation flux (negative bias of reflection) is also found in the Japanese 25-year reanalysis dataset (JRA25) (Trenberth and Fasullo 2010), which is the result of the use of the GSM as the forecast model for JRA25. This report presents a development of the stratocumulus scheme (Sc scheme) aimed at reducing the negative bias in both marine low cloud cover and the reflection of solar radiation at mid-latitudes.

2. Problems in previous versions of the Sc scheme

Kawai (2012a, 2012b) reported that the Sc scheme used in the operational JMA-GSM (Kawai and Inoue 2006) has been improved. The representation of the vertical structure of the subtropical boundary layer clouds was improved, and some of the problems associated with the original version of the scheme were resolved, without recognizable deterioration of the radiation budget.

In the improved scheme, the model conditions necessary to produce Sc are: (1) $\theta_{700} - \theta_{surf} > 20$ [K] (based on Klein and Hartmann 1993); and (2) not stable layer near the surface (to guarantee the existence of a mixed layer). When these two conditions are met, mixing at the top of the cloud layer is completely suppressed to prevent the entrainment of dry air in the free atmosphere into the mixed layer; Additional mixing at the top of the mixed layer, which has been used in the operational model for a long time to prevent the unrealistic formation of clouds at the top of the boundary layer, is not applied, and the lower limit of vertical diffusivity is set to be almost zero at the top of the cloud layer. (Hereafter, this scheme is called the LTS (Lower Tropospheric Stability) Sc scheme.)

However, mid-latitude marine low clouds easily dissipate in this scheme, because LTS cannot have large values in mid-latitudes, so the conditions for the scheme are not met. The left panels in Fig. 1 show the low cloud cover and the TOA shortwave radiation bias of applying the LTS Sc scheme (for January). The mid-latitude low cloud cover is underestimated and the shortwave radiation bias is large, as is

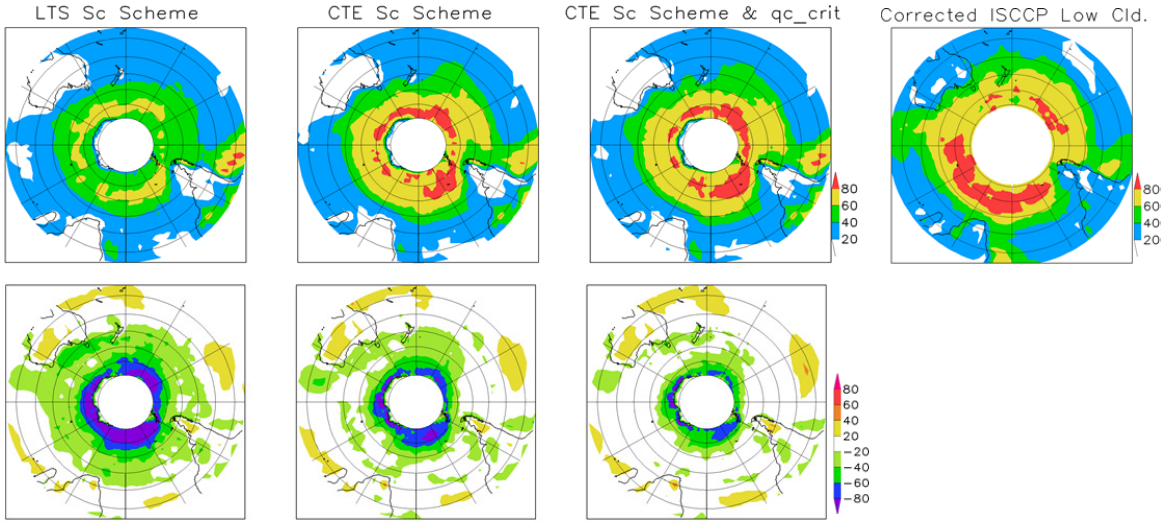

Fig. 1: Top panels: Low cloud cover (%). Bottom panels: Error of TOA upward shortwave flux (W/m^2). The observation data are ERBE. Based on TL159 for January (1987–1989) calculated using the LTS Sc scheme (first from the right), the CTE Sc scheme (second from the right), and with the CTE Sc scheme and the modification of q_{c_crit} (third). The top right panel shows low cloud cover from the ISCCP data, calculated only over areas with no upper clouds.

the case in the operational Sc scheme in the GSM. In addition, the use of LTS in a cloud parameterization can cause an inevitable negative cloud feedback when the model is used for global warming simulations (Wood and Bretherton 2006).

3. Improvement of the Sc scheme

An index EIS (Estimated Inversion Strength) proposed by Wood and Bretherton (2006), which shows relatively large values in mid-latitudes compared with LTS, is basically used in the improved scheme. However, EIS is related only to the inversion strength of (potential) temperature at the cloud top. Consequently, a modified EIS is used here to include the effect of cloud top entrainment (CTE) instability at the cloud top. The most important condition, which is a substitute for the condition (1) of the LTS Sc scheme, is as follows (hereafter, this revised scheme is referred to as the CTE Sc scheme):

$$\mathrm{EIS_{CTE}} = \mathrm{EIS} - (1-k)\,(L/C_p)\,(q_{surf} - q_{700})C_{\Delta q} > 0$$

This is a modification of a criterion of non-CTE instability, $\Delta\theta_e > k(L/C_p)\,\Delta q_t$ (Δ: difference between the values above and below the entrainment zone), which is based on an idea similar to CGLMSE in Kawai and Teixeira (2010). A value of 0.7 is used for k (MacVean 1993), and $C_{\Delta q}$ is the correction factor for the humidity difference whose value is less than 1.0, because Δq_t is actually less than $(q_{surf} - q_{700})$, and $C_{\Delta q} = 0.8$ is assumed here. Fig. 2 shows scatter diagrams of optically thick low cloud cover (presumably, stratocumulus or stratus) and LTS, EIS, and $\mathrm{EIS_{CTE}}$. $\mathrm{EIS_{CTE}}$ has a very high correlation with low cloud cover, at least, at the same level as EIS.

The second panels from the left in Fig. 1 show the results of applying the CTE Sc scheme: mid-latitude low cloud cover increases, being closer to the observation, while the shortwave radiation error decreases. However, there is still a substantial radiation error.

Therefore, the critical cloud water content, from which autoconversion of cloud water to precipitation starts, is increased from 0.2 to 0.4 g/kg in the boundary layer to suppress the excessive conversion of cloud water into precipitation. This change further decreased the radiation error (third panels from the left in Fig. 1).

The impacts of these changes are limited to almost over the mid-latitude oceans where there were large biases of cloud cover and radiation. Furthermore, these changes in the scheme bring the same improvement for Northern Hemisphere mid-latitudes during the summer, which also had the same bias. These improvements can probably be attributed to the fact that the excessive dissipation of cloud water is prevented, and the overly vigorous conversion of cloud water to precipitation is suppressed by these changes.

Acknowledgements

This work was partly supported by the SOUSEI Program of the Ministry of Education, Culture, Sports, Science and Technology (MEXT), and the Research Program on Climate Change Adaptation (RECCA).

References

Kawai, H., 2012a: Examples of mechanisms for negative cloud feedback of stratocumulus and stratus in cloud parameterizations. *SOLA*, **8**, 150-154.

Kawai, H., 2012b: Results of ASTEX and Composite model intercomparison cases using two versions of JMA-GSM SCM. *CAS/JSC WGNE Research Activities in Atmospheric and Oceanic Modelling/WMO*, **42**, 0411-0412.

Kawai, H., and T. Inoue, 2006: A simple parameterization scheme for subtropical marine stratocumulus. *SOLA*, **2**, 17–20.

Kawai, H., and J. Teixeira, 2010: Probability Density Functions of Liquid Water Path and Cloud Amount of Marine Boundary Layer Clouds: Geographical and Seasonal Variations and Controlling Meteorological Factors. *J. Climate*, **23**, 2079–2092.

Klein, S. A., and D. L. Hartmann, 1993: The seasonal cycle of low stratiform clouds. *J. Climate*, **6**, 1587–1606.

MacVean, M., 1993: A Numerical Investigation of the Criterion for Cloud-Top Entrainment Instability. *J. Atmos. Sci.*, **50**, 2481–2495.

Trenberth, K. E., and J. T. Fasullo, 2010: Simulation of Present-Day and Twenty-First-Century Energy Budgets of the Southern Oceans. *J. Climate*, **23**, 440–454.

Wood, R., and C.S. Bretherton, 2006: On the Relationship between Stratiform Low Cloud Cover and Lower-Tropospheric Stability. *J. Climate*, **19**, 6425–6432.

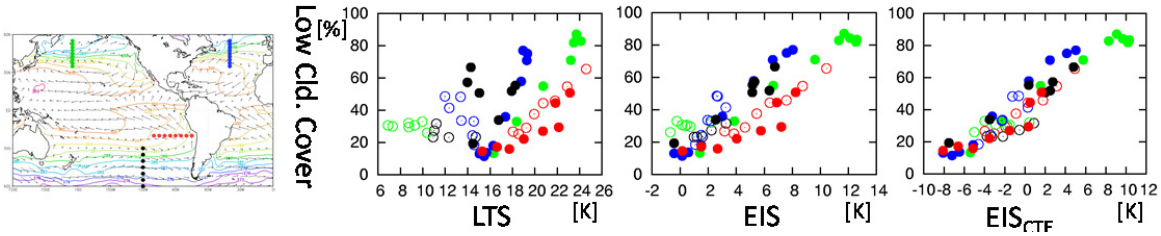

Fig. 2: Left panel shows the data locations. Other panels show scatter diagrams of low cloud cover (%) and LTS (second from the left), EIS (third), and $\mathrm{EIS_{CTE}}$ (fourth). Low cloud cover in these panels is calculated from the ISCCP low cloud data whose optical depth is greater than 3.55 only over areas with no upper clouds. Data are from January and July 1999–2001. Solid circles correspond to summer data, and open circles to winter. For $\mathrm{EIS_{CTE}}$, k = 0.7 and $C_{\Delta q} = 0.8$ are used.

PCMT :
Prognostic Condensates Microphysics and Transport
A new convection scheme for the global Climate and NWP model ARPEGE

Jean-Marcel Piriou and Jean-François Guérémy
Météo-France CNRM/GAME
jean-marcel.piriou@meteo.fr, jean-francois.gueremy@meteo.fr

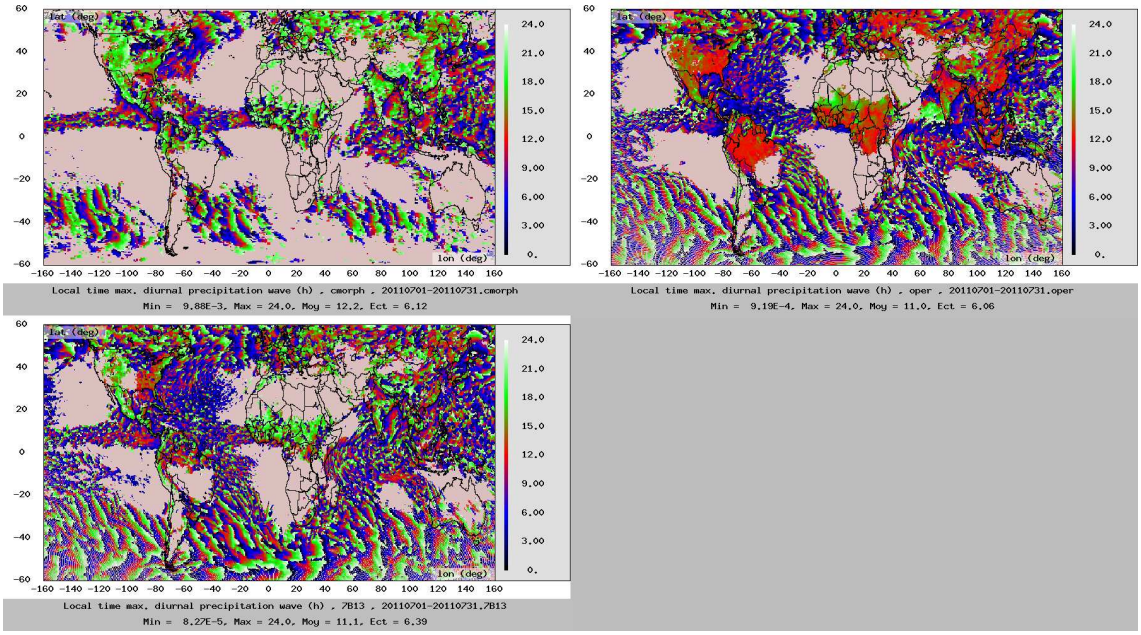

PCMT (Prognostic Condensates Microphysics and Transport) is a convection scheme under development, to provide better sensitivity to environmental humidity, through 4 prognostic variables (liquid water, ice water, rain, snow). The vertical velocity equation is also prognostic. The grid-scale equations from the convection scheme separate microphysical processes and transport processes, after (Piriou et al., 2007). The prognostic microphysics is taken from (Lopez, 2000), entrainment and closure of the scheme from (Guérémy, 2011). The vertical transport of udpdraft species is done by an unconditionnally stable algorithm, following (Geleyn et al., 2008). One of the objectives is to increase the sensitivity of model convection to environmental humidity.

As an example, the liquid water equation stands

$$\begin{aligned}\frac{\partial}{\partial t}\overline{q_{lc}} &= \text{Advec}(\overline{q_{lc}}) \\ &\quad -\frac{1}{\rho}\frac{\partial}{\partial z}\rho\left[\alpha_u w_u + \alpha_d w_d\right] q_{lc} \\ &\quad +\left(E_u + E_d\right) q_{lr} - \left(D_u + D_d\right) q_{lc} \\ &\quad +\text{CondensEvap}_{q_{lc}} - \text{AutoconvColl}_{q_{lc}} + \text{MeltingIcing}_{q_{lc}}\end{aligned} \tag{1}$$

where Advec($\overline{q_{lc}}$) is resolved 3D advection, α is the surface of draft, u stands for updraft, d for downdraft, w is vertical velocity, E entrainment, D detrainment, q_{lc} convective liquid

water, on the fourth line are the three microphysical processes condensation-evaporation, autoconversion-collection, melting-icing.

The above figure presents some results obtained with the PCMT scheme on the diurnal cycle of convective precipitation, as simulated by two versions of the global NWP model ARPEGE of Meteo France :

1. The upper left panel shows the observed precipitation timing (local time when precipitation rate is a maximum) computed on the basis of the NOAA CMORPH analysis data set. The data are averaged over one month, viz., July 2011. Over land, the precipitation rate peaks in late afternoon as indicated by green colours. Over much of the World Ocean, the signal is weak, and no conclusive statement can be made.
2. The upper right panel shows the results from simulation with the standard version of ARPEGE used operationally at Meteo France. As in many other global NWP models, precipitation rate peaks around local noon, i.e. too early as compared to observations.
3. The lower left panel shows the results from ARPEGE simulation, where the standard ARPEGE cumulus convection scheme is replaced by the PCMT scheme. As seen from the plot, the timing of precipitation maximum is clearly improved over many regions, e.g. over Central Africa, India, Amazonia, Mexico, and United States.

Références

Courtier, P., Freydier, C., Rabier, F., and Rochas, M. (1991). The ARPEGE project at Meteo-France,Numerical methods in atmospheric models. *ECMWF Seminar Proceedings*, 2 :193–231.

Geleyn, J.-F., Bazile, E., Bougeault, P., Déqué, M., Ivanovici, V., Joly, A., Labbé, L., Piedelièvre, J. P., Piriou, J.-M., and Royer, J.-F. (1995). Atmospheric parametrization schemes in Météo-France's ARPEGE N. W. P. model. In *Proceedings of the 1994 ECMWF seminar on physical parametrizations in numerical models*, pages 385–402. ECMWF.

Geleyn, J.-F., Catry, B., Bouteloup, Y., and Brozkova, R. (2008). A statistical approach for sedimentation inside a microphysical precipitation scheme. *Tellus*, 60(4) :649–662.

Guérémy, J.-F. (2011). A continuous buoyancy based convection scheme : one- and three dimensional validation. DOI 10.1111/j.1600-0870.2011.00521.x. *Tellus*, 63A :687–706.

Lopez, P. (2000). Implementation and validation of a new prognostic large-scale cloud and precipitation scheme for climate and data-assimilation purposes. *Quart. J. Roy. Meteor. Soc.*, 128 :229–257.

Piriou, J.-M., Redelsperger, J.-L., Geleyn, J.-F., Lafore, J.-P., and Guichard, F. (2007). An approach for convective parameterization with memory : separating microphysics and transport in grid-scale equations. DOI 10.1175/2007JAS2144.1. *J. Atmos. Sci.*, 64(11) :4127–4139.

Development of longwave radiation scheme with consideration of scattering by clouds in JMA global model

Syoukichi Yabu

Meteorological Research Institute / Japan Meteorological Agency , Tsukuba

E-mail: syabu@mri-jma.go.jp

1. Introduction

Current version of longwave radiation (LW) scheme in the MRI/JMA global atmospheric model calculates only absorption and emissivity process due to the atmospheric molecules, aerosol particles and clouds. Clouds, including thin ice clouds, are approximated with black bodies (Räisänen,1998) in this scheme. In addition, it is used band-emissivity method to calculate the LW radiative transfer, which takes computational cost proportional to almost square of number of vertical layers of the model, so it makes a matter in increasing the vertical resolution of the model. In order to improve these drawbacks, new LW scheme has developed which is able to consider LW scattering by clouds and is also able to calculate the radiative transfer more efficiently.

2. New longwave radiation scheme

2 or 4-stream radiation transfer method is applied in the new LW scheme. According to Li & Fu (2000), two types of schemes are implemented; one is the absorption approximation version, referred as AA, which do not consider scattering process like as the current JMA LW scheme, and the other is a version considering scattering process, referred as AAS. In the radiative transfer equation of the AAS version, the source term by scattering is evaluated with using the radiative intensity of the AA solution. As Li & Fu argued, it is confirmed that this treatment of LW scattering has advantages in both the efficiency and the accuracy of the calculation.

In the new LW scheme, absorptions due to the atmospheric molecules are calculated by two types of k-distribution methods. One is the correlated k-distribution method (i.e. Fu and Liou,1992) where the absorption coefficients at 51 pressure levels between 1000 and 0.01hPa are tabulated by using the HITRAN(2000) absorption line database. The other is referred as a "scaling" k-distribution method (i.e. Chou et al.,2001), used also in the current JMA LW scheme, where the Lorentzian line absorption (pressure broadening) is assumed and only one absorption coefficient at a specified pressure level (500hPa) is prepared.

Table 1 shows calculation bands and variation of absorption gas molecules in the new scheme, with denoting k-distribution types and number of sub-bands, also denoting the overlap assumption of absorptions in the same band. The correlated k-distribution method (C-k, or blue colored) is applied to the absorptions important in the stratosphere, that is CO_2 in the 15 micron band, O_3 in the 9.6 micron band and H_2O in the three bands. The "scaling" k-distribution method (S-k, or yellow colored) is applied to the other absorptions, including H_2O continuum based on MT-CKD continuum model and Zhong & High (1995) scaling parameters. Number of sub-bands used in S-k is not larger than 6, enough to approximate absorptions in the troposphere, whereas number of sub-bands used in C-k is set to 16, required to represent a sharp peak of the Doppler type absorption line appeared in the stratosphere or higher atmosphere. Overlap assumption of each band/absorption is selected from the following three types: perfect, random and partly correlated (Zhang et al.,2003), except for overlap between CO_2 and H_2O in the 15-micron band (band3a-3c) treated by considering CO_2 and H_2O as one combined virtual gas.

3. Verification of the new scheme

Figure 1 shows heating rate profiles calculated by the new LW scheme compared to the current JMA scheme and Line by Line reference calculation. Observed atmospheric profiles used here are taken from CIRC project (Oreopoulos & Mlawer 2010). Upper two figures indicate that the new scheme has better calculation accuracy for clear sky conditions than the current scheme in general, especially in the upper troposphere and the higher region. From the right figure (high precipitable water case), there may be room for improvement on the scheme in the lower troposphere (evaluation of water vapor continuum absorption). Lower two figures are for the case of existing liquid cloud layer (no scattering condition). It is ascertained generally good calculation is performed for the two cases. Although slightly strong radiative cooling is seen around the top of cloud layers, it may be caused by the parameterization to derive optical depth of cloud layers from the effective radius of cloud particles.

4. Application to the global atmospheric model

New LW scheme has implemented to the JMA global atmospheric model (GSAM). 2AA (2-stream AA) version of the scheme has larger effect on the shortwave radiation (SW) field in the model than on the LW field. Figure 2 indicates the effect about SW radiative flux at the surface (in July). The red shade in the center figure indicates 2AA model improves insufficiency of the downward SW flux on the subtropical ocean of GSAM, shown in the left figure. Although 2AA and the GSAM LW scheme are the same as to having no scattering process, 2AA tends to give weaker cooling in the clear-sky lower troposphere than GSAM. It brings to decrease of low cloud amount (the right figure) and contributes to weaken the reflection of SW by clouds. Another difference has confirmed in the atmospheric temperature in the stratosphere (not shown here), due to the difference of heating rates in the clear-sky condition (already shown in Fig.1).

On the other hand, LW scattering has smaller effect on the model climate than expected. From 10 case model experiment, monthly mean OLR difference between 4AAS (4-stream AAS) and 4AA (4-stream AA) version is less than 5 W/m^2 in the globe, though difference of estimated OLR for the same atmospheric field is often seen larger than 10 W/m^2, especially around Japan and west of the continents. Finally, computation speed has measured with TL159L60 resolution model on Hitachi SR16000 supercomputer system. The result is that 2AA model is about 10% faster than GSAM (55% of computational time of GSAM for the radiation section) and even for 4AAS model, it takes almost the same computational time as GSAM.

Table 1: band configuration of new LW scheme
(pf,pt and no in each parenthesis denote perfect, partly and random overlap assumption, respectively)

# band	1	2	3a	3b	3c	4	5	6	7	8	9
wave no. (/cm)	(25-340)	(340-540)	(540-620)	(620-720)	(720-800)	(800-980)	(980-1100)	(1100-1215)	(1215-1380)	(1380-1900)	(1900-3000)
Major absorption gas											
H2O (line)	C-k (16)		C-k (16,cg)			S-k (6)	S-k (6,pf)	S-k (16,pf)	S-k (4)	C-k (16)	S-k (6)
CO2											
O3							C-k (16)	C-k (16)			
H2O (continuum)	S-k (16,pt)					S-k (6,pf)		S-k (16,pf)	S-k (4,pf)	S-k (pt,16)	S-k (6,pf)
minor absorption gas											
CO2						S-k (6,pf)					
N2O			S-k (6,pf)					S-k (16,pf)	S-k (2,no)		
CH4									S-k (2,no)		
CFCs						S-k (6,pf)					
# of sub-bands	16	16	16	16	16	6	16	16	16(=4x2x2)	16	6

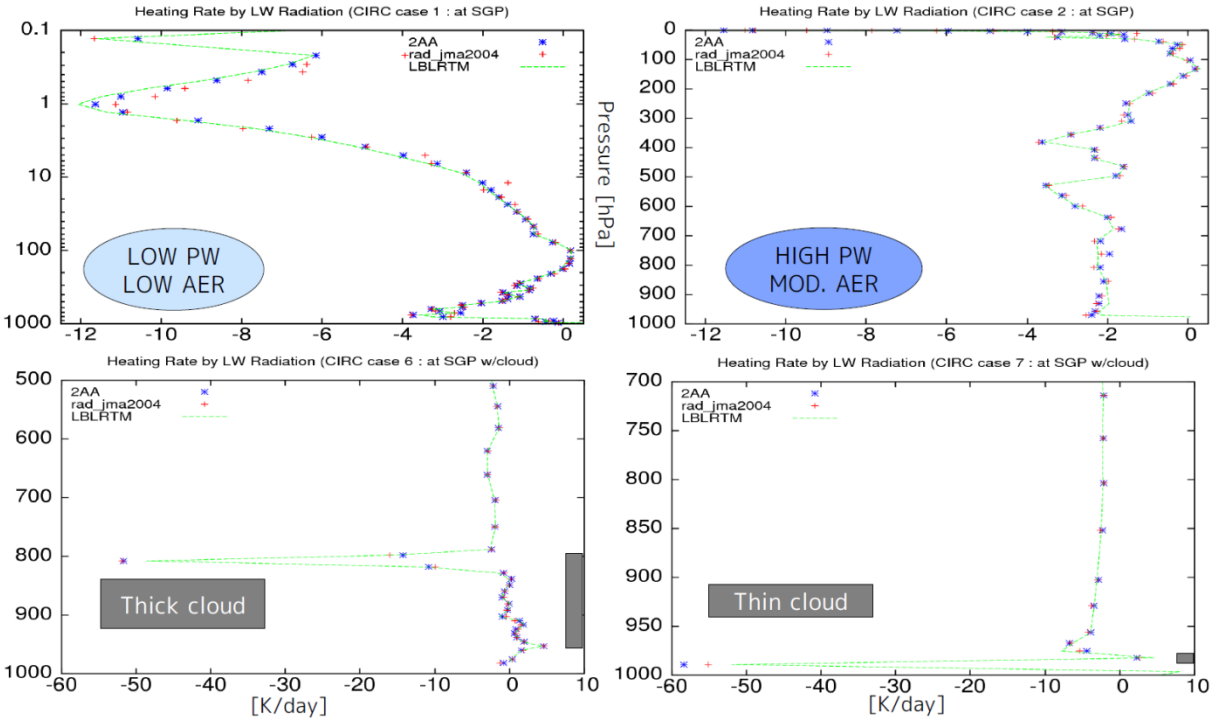

Figure 1: Heating rate profiles for the CIRC atmospheric profiles. PW and AER denotes precipitable water and aerosol. Blue and red dots are calculated by 2AA and the current scheme. Green lines indicate LBL reference calculations. Water cloud layers are located in the heights illustrated by the gray boxes at the far right of the lower two figures.

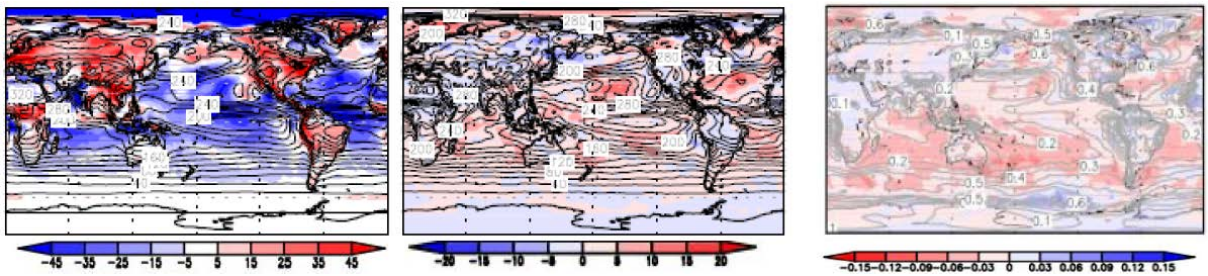

Figure 2: Downward SW flux at the surface in July. (left) flux difference of GSAM from observed(CERES) climatology. (center) flux difference of 2AA from GSAM. (right) difference of modeled low cloud amount between 2AA and GSAM. Unit of SW flux is W/m^2. The model forecasts (2AA and GSAM) are an average on 10 year cases.